ISSN 1063-7826, Semiconductors, 2015, Vol. 49, No. 12, pp. 1550–1556. © Pleiades Publishing, Ltd., 2015.
Original Russian Text © A.P. Protogenov, E.V. Chulkov, 2015, published in Fizika i Tekhnika Poluprovodnikov, 2015, Vol. 49, No. 12, pp. 1598–1604.

XIX SYMPOSIUM "NANOPHYSICS AND NANOELECTRONICS", NIZHNY NOVGOROD, MARCH 10–14, 2015

Universal Properties of Materials with the Dirac Dispersion Relation of Low-Energy Excitations

A. P. Protogenov[a]* and E. V. Chulkov[b,c,d]

[a] *Institute for Applied Physics, Russian Academy of Sciences, ul. Ul'yanova 46, Nizhny Novgorod, 603950 Russia*
[b] *Departamento de Fisica de Materiales, Universidad del Pais Vasco, 20080 San Sebastian/Donostia, Spain*
[c] *Saint Petersburg State University, ul. Ul'yanovskaya 3, Staryi Peterhoff, St. Petersburg, 198504 Russia*
[d] *National Research Tomsk State University, pr. Lenina 36, Tomsk, 634050 Russia*
* *e-mail: alprot@appl.sci-nnov.ru*

Submitted April 22, 2015; accepted for publication May 12, 2015

Abstract—The *N*-terminal scheme is considered for studying the contribution of edge states to the response of a two-dimensional topological insulator. A universal distribution of the nonlocal resistance between terminals is determined in the ballistic transport approach. The calculated responses are identical to experimentally observed values. The spectral properties of surface electronic states in Weyl semimetals are also studied. The density of surface states is accurately determined. The universal behavior of these characteristics is a distinctive feature of the considered Dirac materials which can be used in practical applications.

DOI: 10.1134/S1063782615120143

1. INTRODUCTION

Topological insulators and Weyl semimetals are characterized by the linear dispersion of low-energy excitations existing at the edge of two-dimensional topological insulators or on the surface of three-dimensional topological insulators, and in the bulk of Weyl semimetals. Such electronic states have helicoidal spin orientation, and the spin orientation is related to the direction of electron momentum. The electronic states in topological insulators [1–3] are protected by time-reversal symmetry, which leads to topological protection of each Kramers partner and as a result to the suppression of backscattering in systems with moderate structural disorder. The distinctive feature of a Weyl semimetal is that this three-dimensional material exhibits a conical spectrum near an even number of points in momentum space, where the bands touch each other.

The features of topological insulators manifest themselves even for nanoscale samples. Indeed, topological order in topological insulators belongs to the phase state with so-called short-wavelength order [4], which is created by correlated quantum states on scales on the order of the lattice constant. The topological phase formed on large scales, so-called long-wavelength topological order, belongs to a fundamentally different class [4] formed by correlated quantum states. One of its features is nonlocality in the Hilbert space of states. This means that the full quantum state is not equal to the product of local electronic states. In other words, this state contains long-wavelength correlations of topological excitations.

Nontrivial topological order has an effect on the electron collision frequency [5]. The Berry phase of quantum states in topological insulators appears in interference phenomena and leads to the weak antilocalization phenomenon [6]. In Section 2, we consider the universality of the transport characteristics of two-dimensional topological insulators under conditions when they contain information on nonlocal topological order. The existence of nonlocality in the three-dimensional case follows directly from the representation [7] of the topological invariant. The nontrivial value of this Hopf invariant equal to unity means that two loops are linked. In this paper, we focus on studying the significantly nonlocal response detected in experiments [8, 9].

2. NONLOCAL RESPONSE

The features of electronic states in two-dimensional topological insulators manifest themselves in the quantum-spin Hall effect [10–13]. In studying the degree of nonlocality, we use the approach of [8, 14] generalized to the case of the *N*-terminal scheme. Let us consider the distribution of voltages between terminals of the *N*-terminal scheme, caused by edge states in a two-dimensional topological insulator. In the Landauer–Büttiker ballistic transport approach [15,

16], the current injected through terminal i to the sample is given by

$$I_i = \frac{e^2}{h}\sum_{j=1}^{N}(T_{ji}V_i - T_{ij}V_j), \quad (1)$$

where V_j is the terminal j potential, e is the elementary charge, h is Planck's constant, h/e^2 is the measurement unit of the fundamental resistance which we further set to unity, T_{ij} is the matrix element of the transition from terminal i to terminal j, and N is the total number of terminals.

In the general case, the transition coefficients T_{ij} depend on the potentials V_j and geometrical parameters of the problem. We will consider the situation of maximum resistance, experimentally implemented in [8], when it can be considered that the transition coefficients T_{ij} are independent of potentials V_j. In this case, the bulk Fermi level is at the energy-gap center, and the renormalized voltage $V^* = 0$ [8]. The relations between the characteristic sizes of the terminal and sample are considered at the end of the Section in discussing deviations from the ideal limit under study. Taking into account that edge electronic modes in topological insulators propagate in two mutually opposite directions, let the coefficients of the transition between the nearest terminals in this ideal case be unity, $T_{i+1,i} = T_{i,i+1} = 1$, and other coefficients be zero. Furthermore, the N-terminal scheme implies that the periodic boundary conditions $T_{N+1,N} = T_{1,N}$, $T_{N,N+1} = T_{N,1}$ take place for both propagation directions of edge states.

Let us consider the number of terminals N as the control parameter. The indices of terminals between which we will measure voltage, contain information about the effect of the current of edge states between terminals through which it flows on the distribution of voltage at other terminals. This distribution defines the degree of response nonlocality. It is clear that the resistance between terminals with indices 1 and N, through which the current flows, will tend to unity with increasing number of terminals N. For example, in the case of adjacent terminals with indices 1 and 2, the measured resistance will tend to zero by some law with increasing N.

Let the current I_{1N} flow through terminals 1 and N, and the voltage be measured at terminals with random indices i and j. In this case, the equation defining the potentials between terminals is written as

$$AV = I, \quad (2)$$

where $A_{ij} = 2\delta_{ij} - \delta_{i,j+1} - \delta_{i,j-1} - \delta_{i,1}\delta_{j,N} - \delta_{i,N}\delta_{j,1}$, δ_{ij} is the Kronecker delta, $1 \leqslant i, j \leqslant N$, $V = (V_1, V_2, \ldots V_{N-1}, V_N)$, and $I = I_{1N}(1, 0, \ldots 0, -1)$. Our interest is in the difference between the terminal potentials V_i. Since the vector V is invariant with respect to a constant-value shift, we can set $V_N = 0$.

For arbitrary N, the solution to Eq. (2) is $V_i = I_{1N}(1 - i/N)$. Therefore, the resistance $(V_1 - V_N)/I_{1N}$ between terminals with indices 1 and N is $R_{1N,1N} = (N-1)/N$. The nonlocal resistance $R_{kl,ij} = (V_i - V_j)/I_{kl}$ at $k = 1$, $l = N$ in measuring the voltage between terminals i and j in this more general case is

$$R_{1N,ij} = \frac{j-i}{N}. \quad (3)$$

To find the voltage distribution in the case where the current flows from terminal 1 to terminal k, it is necessary to use the expression for the current $I = I_{1k}(1, 0, \ldots -1, \ldots 0)$ on the right-hand side of (2). Here -1 is at the k-th point. In this general case, the exact solution to Eq. (2) is given by

$$V_i = I_{1k}\left[1 - \frac{i}{N}(1 - k + N)\right], \quad (4)$$

if $1 \leqslant i \leqslant k$, and

$$V_i = I_{1k}\left(1 - \frac{i}{N}\right)(1 - k), \quad (5)$$

if $k \leqslant i \leqslant N$. Such a distribution of indices of the current terminal and terminals at which voltages are read, defines the following resistances

$$R_{1k,ij} = \begin{cases} \dfrac{j-i}{N}(1-k+N), & 1 \le i, j \le k, \\ \dfrac{j-i}{N}(1-k), & k \le i, j \le N, \\ \dfrac{j-i}{N}(1-k) + (k-i), & 1 \le i \le k, k \le j \le N. \end{cases} \quad (6)$$

After permutation of the current terminal indices $(1k)$ and indices (ij) of the terminals at which voltages are read, and after shifts $k \to j - i + 1$, $j \to k - i + 1$, $i \to N - i + 2$, we can verify that these expressions satisfy the Onsager–Casimir symmetry relations $R_{mn,kl} = R_{kl,mn}$ for nonlocal resistances $R_{mn,kl}$. We note the fact that the universality of ballistic edge-state transport under the considered ideal conditions is controlled by the topological properties of bulk quantum electronic states. Therefore, this phenomenon is lacking in trivial insulators.

We considered the universal properties of nonlocal transport existing due to helicoidal edge electronic modes propagating along the edge of a two-dimensional topological insulator in two mutually opposite directions. Violation of the indicated equivalence corresponds to the chiral situation. This takes place in the case of the violation of time-reversal symmetry. If the time-reversal symmetry is violated, e.g., due to the introduction of magnetic impurities, and the condition that backscattering is lacking is weakened, the transition coefficients $T_{i,j}$ can be written as $T_{i+1,i} = 1 + k_1$, $T_{i,i+1} = k_2$ [17]. Here $k_1 < 1$ and $k_2 < 1$ are constants, and unity in the transition coefficient $T_{i+1,i}$

means the existence of the chiral edge mode. In this quasi-helicoidal edge state [17], the distribution of potentials at terminals with the index i, if the current flows through terminals 1, N to which voltage is applied, has the exponential form

$$V_i = \left(\frac{1-r^{N-i}}{1-r^N}\right)\frac{I_{1N}}{1+k_1}, \quad (7)$$

where $r = k_2/(1 + k_1)$.

Chiral edge states in the quantum Hall effect propagate only in one of two possible directions. The transition coefficients for such states in Eq. (1) are nonzero for terminals with indices $j > i$: $T_{i,i+1} = 1$ and $T_{i+1,i} = 0$. Therefore, the resistance $R_{1N,ij}$ appears equal to zero. In other words, nonlocal resistance in systems with violated time-reversal symmetry is absent. The existence of such symmetry at the macroscopic level appears as nonlocal effects caused by helicoidal edge states. The shape of responses and determined numbers before the factor h/e^2 in the resistance depend on the experimental conditions, e.g., on the temperature which controls the contribution to the conductance of inelastic backscattering processes. The experimental data [8] exhibit a high degree of universality. The universality of expressions $R_{1N,1N} = (N - 1)/N$, $R_{1N,ij} = (i - j)/N$ and (4), (5) can be tested using experimental setups for studying the quantum-spin Hall effect through varying the total number of terminals and indices of current-carrying terminals.

In this paper, we focus on the universal manifestation of topological order in the transport properties of ideal two-dimensional topological insulators in the simplest form of its representation. Studying the transport characteristics of topological insulator SmB_6 shows [9] that transport properties in the three-dimensional case depend heavily on the sample configuration and terminal distribution. The deviation from universal behavior takes place in two-dimensional systems as well. It results from metal droplets within real terminals. This phenomenon can be described in terms of an additional terminal. The effect of this and other factors such as finite terminal size, reflection from the inner boundaries, and other conditions on the amplitudes of the transitions between current terminals and test terminals from which voltages are read was studied in [18].

Let us clarify in more detail the role played by terminals in edge-state transport, following the approach and main conclusions of [8, 18, 19]. We first note that terminals are not potentials which violate time-reversal symmetry, which mix oppositely propagating edge states with oppositely oriented spins. After all, terminals represent a reservoir of electronic degrees of freedom with incoherently populated channels of both edge states. An ideal terminal populates both channels of edge states with the same weight, injecting spin-up and spin-down electrons with equal probability [8]. This is the cause of the additional resistance induced by terminals. The contribution of such a dephasing reservoir to the additional resistance can be negligible under the condition that $L < L_c \sim 1/\eta$. Here L is the characteristic linear size of the terminal, L_c is the dephasing length, η is the dephasing term in the intrinsic energy [8]. We note that the intrinsic energy should not violate time-reversal symmetry. The decoherent behavior is caused by the existence of the dephasing reservoir with the distribution function included in the so-called low intrinsic energy of the terminal [8].

However, deep dips in the conductance exist even at small parameters ηL. They can be sufficiently strong to completely suppress coherent transport at one of the edges [8]. Therefore, even a small dephasing region can significantly affect the test terminal. The experimental value of the maximum resistance for a 6-terminal scheme is 1/7 instead of the theoretical prediction of 1/6. Such a result is consistent with the existence of an additional dephasing region. Dephasing regions can also exist due to sample inhomogeneity. The experimental results show [8] that a change in the output voltage also affects the sample heterogeneity due to occupied states gaining a charge at the semiconductor–insulator interface. This results in a nonuniform potential in the region of terminals and the formation of metal islands which exist, even when most terminal regions are insulating. In other words, the metal island can cause an effect similar to the existence of an additional test terminal. Experimental situations when coherent transport is observed in the entire sample were discussed in [8, 18].

There are two different methods for suppressing nonlocal transport. The first approach is as follows: the sample scale is made so small that it induces backscattering in the edge-state channels. Backscattering occurs if wave functions for the opposite spin orientation are overlapped [20]. This occurs in a sample 200 nm wide. Therefore, if the width of the central region of a two-dimensional sample strip satisfies the condition $W > W_1$, i.e., is rather large, the deviation T'_{1N} from the ideal value $T_{1N} = 1$ is negligible [18]. The same condition $W > W_2$ for the absence of tunneling between edges of an individual terminal is valid for the terminal width W_2. Measurements of the nonlocal resistance [18] in samples being in states of the quantum-spin Hall effect yield values expected for nonperturbative nonlocal transport over edge states. Numerical calculations of the scattering matrix at the metal–topological-insulator interface confirmed the negligible values of T'_{1N} for the used samples. The second method for suppressing the contribution to nonlocal edge-state transport consists in the selection of such nonlocal configurations which assume transport via the edge channel to distances larger than the inelastic scattering length [19]. This means that the largest number of terminals $N_c = L_1/(W_2 + L_2)$ can be

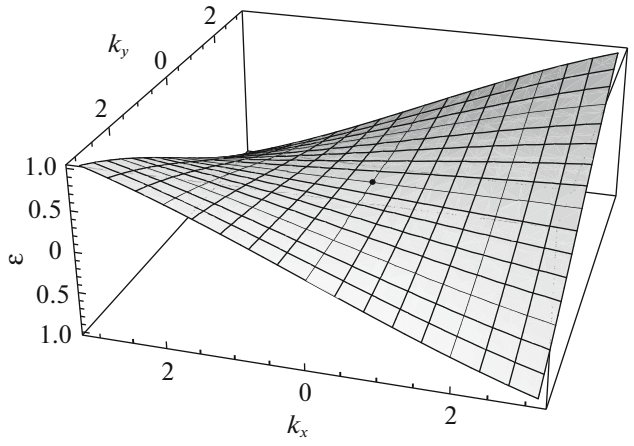

Fig. 1. Spectrum of surface states in the Weyl semimetal. The dot is the origin of coordinates $k_x = k_y = 0$.

roughly estimated as 10 for actual experimental parameters. Here L_1 is the characteristic size of the sample and L_2 is the distance between terminals.

Finally, it should be noted that we described the universal distribution of resistances, studying the nonlocal transport of edge states in two-dimensional topological insulators in the ballistic mode. It is of interest to study problems of the macroscopic manifestation of topological order in other topologically ordered systems. An important problem in this field lies in simulation [21] of the distribution of degrees of freedom in systems with long-wavelength topological order. In this case, instead of *H*-shaped basic elements of the scheme used in this study, we should use *Y*-shaped terminals as building blocks.

3. DENSITY OF SURFACE STATES

In this Section, we consider the spectral properties of surface electronic states in Weyl semimetals. A necessary condition for the existence of Weyl semimetals is violation of the spatial inversion or time-reversal symmetry. The topological protection of bulk quantum states of this three-dimensional analogue of graphene appears in the form of surface states belonging to Fermi arcs in momentum space. Therefore, studying the properties of surface electronic states which are characteristic features of hidden topological order in three-dimensional systems with the conical spectrum near Weyl points, allows the clarification of some symmetry aspects of topological protection of three-dimensional quantum states.

A remarkable feature is that Weyl points in momentum space are monopoles with topological charges equal to the first Chern invariant [22, 23]. The existence of an even number of Weyl points characterized by alternating opposite-sign monopole charges, hence, zero total topological charge, allows the following conclusion. The bulk spectrum of electronic states in Weyl semimetals at finite-energy distance from Weyl points necessarily has the hyperbolic shape. This means that the surface spectrum projected on the two-dimensional Brillouin zone will reflect the indicated hyperbolicity: it will contain disconnected one-dimensional dispersion distributions in the form of Fermi arcs, when the dispersion relation of surface states is sectioned by the constant energy at the Fermi level. Summarizing, we can say that the cause of the existence of Fermi arcs is the hidden topological behavior of bulk electronic-state phases in Weyl semimetals.

The class of materials for implementing Weyl semimetals includes TaAs [24, 25], heterostructures constructed from topological and conventional insulators [26], and topological insulators doped with magnetic impurities [27]. Currently, the topological classification [22, 28–30] of phase states in topological insulators is extended to Weyl semimetals [31]. The nontrivial values of topological invariants allow materials containing Weyl points to exhibit a wide spectrum of new phenomena. Recently, the transport features [32, 33] of semimetals, associated with the existence of a chiral anomaly in these media [34], were studied, as well as the spectrum of collective excitations [35, 36], negative magnetoresistance [37], nonlocal transport [38], anomalous quantum Hall effect [39], and extraordinary superconductivity [40] and other phenomena [41, 42] were detected. Friedel oscillations due to Fermi arcs in Weyl semimetals were studied in [43], where the contribution of bulk and surface states to the density of surface states in the model of alternating band and topological insulators was calculated. Surface-state-density oscillations in Weyl semimetals in a strong magnetic field and their experimentally verified results were studied in [44, 45].

We consider properties of Weyl semimetals in the case where there is time-reversal symmetry, and spatial inversion is violated [46], focusing on the study of the density of surface states. This type of Weyl semimetal was studied in [47], where the spectrum of surface states was obtained. It is given by

$$E(k_x, k_y) = 4t \sin\frac{k_x a}{4} \sin\frac{k_y a}{4} \tag{8}$$

and is shown in Fig. 1. Here $k = (k_x, k_y)$ is the two-dimensional wave vector, t is the amplitude of hopping to neighboring lattice sites, and a is the lattice constant.

Figure 2 shows the Fermi arcs obtained by sectioning the surface $E(k_x, k_y) = E$ at a level of $E = 0.2t$. The density of surface states is defined by the integral over the surface Brillouin zone (BZ) $|k_x \pm k_y| \leqslant 2\pi/a$, i.e., the function $\delta[E - E(k_x, k_y)]$ as follows

$$N(E) = \int_{\mathrm{BZ}} \frac{d^2k}{(2\pi)^2} \delta[E - E(k_x, k_y)]. \tag{9}$$

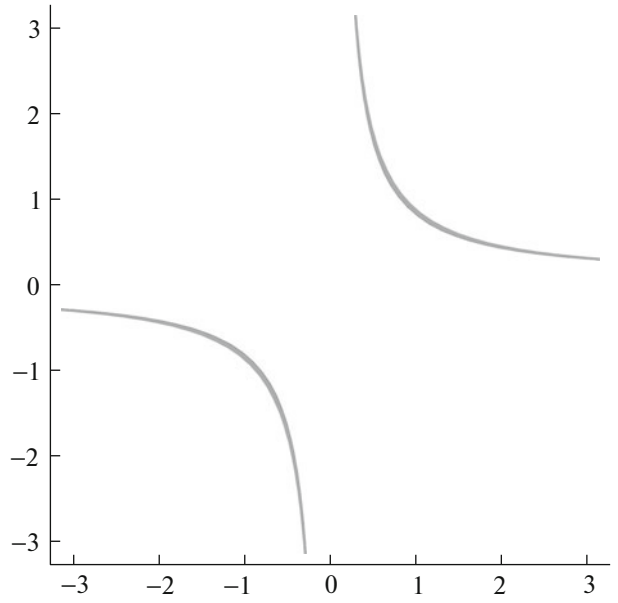

Fig. 2. Fermi arcs at $\varepsilon = 0.1$.

After introducing dimensionless quantities, i.e., the density of surface states $n(\varepsilon) = N(E)/N_0$, $V_0 = 4/(\pi^2 a^2 t)$, the energy $\varepsilon = E/2t$, wave-vector components $(x, y) = (k_x a/4, k_y a/4)$, and after changes in the variables $\xi = x - y$, $\eta = x + y$, we obtain

$$n(\varepsilon) = \frac{1}{4}\int\limits_{-\pi/2}^{\pi/2} d\xi \int\limits_{-\varepsilon}^{\varepsilon} d\eta\, \delta[\varepsilon - \cos\xi + \cos\eta].$$

After changing the integration variables in this expression, the second step reads the δ-function, and the third step leads to the first-order Legendre elliptic integral

$$n(\varepsilon) = \int\limits_0^{1-\varepsilon} \frac{dt}{\sqrt{(1-t^2)[1-(\varepsilon+t)^2]}} = \int\limits_0^{\varphi} \frac{d\alpha}{\sqrt{1-m\sin^2\alpha}} = F(\varphi, m). \quad (10)$$

The amplitude $\varphi = \arcsin\sqrt{2(1-\varepsilon)/(2-\varepsilon)}$ and the parameter $m = 1 - (\varepsilon/2)^2$ of the elliptic integral of the first kind $F(\varphi,m)$ depends on an energy ε in the range $0 < \varepsilon < 1$. The asymptotic values of the elliptic integral of the first kind define the behavior of the density of surface states for $\varepsilon \to 0$ and $\varepsilon \to 1$ as

$$n(\varepsilon) = \begin{cases} \ln\tan(\pi/4 + \varphi/2), & \varepsilon \to 0\,(\varphi \to \pi/2), \\ \sqrt{2(1-\varepsilon)}, & \varepsilon \to 1. \end{cases} \quad (11)$$

The density of surface states as a function of energy ε in the range $0.1 < \varepsilon \leqslant 1$ is shown in Fig. 3.

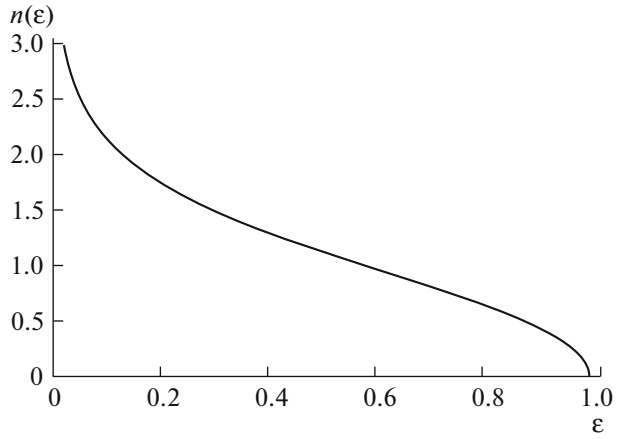

Fig. 3. The density of surface states $n(\varepsilon)$ as a function of energy ε in a Weyl semimetal.

It should be noted that expression (10) for the density of surface states is applicable to the energy range $\varepsilon_1 < \varepsilon < \varepsilon_2$ with $\varepsilon_1 > 0$ and $\varepsilon_2 < 1$ until surface states merge with the continuum of bulk electronic states [47]. In other words, the energy range belonging to surface states at moderate violation of the reversal symmetry is smaller than the interval (0, 1).

The density of states is defined by the electron-spectrum dispersion and the spatial dimension d of the problem at hand. In general, the density of states is a non-decreasing function of energy. An exception is the one-dimensional case with the quadratic spectrum $E_p = p^2/2m_e$, when $N(E) \propto E^{-1/2}$. For comparison, the density of surface states in topological insulators is $N(E) = E/(2\pi h^2 v_F^2)$, whereas for bulk states in Weyl semimetals, it has the form $N(E) = E^2/(2\pi^2 h^3 v_F^3)$, where v_F is the Fermi velocity. The phase-space constraint affects the contribution to thermodynamic characteristics, e.g., decreases the specific heat $C \propto T^d$ (T is the temperature and $d = 2, 3$) for Dirac materials. In the considered two-dimensional problem, the reason that the function $n(\varepsilon)$ is a decreasing function is associated with the existence of a saddle point at the center of the surface Brillouin zone. The latter leads to the appearance of the van Hove singularity at $\varepsilon \to 0$. The further decrease in the function $n(\varepsilon)$ at $\varepsilon \to 1$ reflects the decrease in the Fermi-arc length. As a result, in the intermediate energy region, the surface-state density appears to greater resemble the behavior of this function for a system of two one-dimensional mutually perpendicular Dirac metals, than its behavior in the case of two-dimensional Dirac metal, when $n(\varepsilon) \propto \varepsilon$. This note is consistent with the published observation [48–50] that the system of Dirac surface electronic modes can be considered as a composition of orthogonal Luttinger one-dimensional metal conductors.

Knowledge of the function $n(\varepsilon)$ and its value $n(\varepsilon_F)$ at the Fermi energy ε_F makes it possible to find the quantum capacitance $C_Q = e^2N(\varepsilon_F)$ in a two-dimensional system per unit area, and to determine the contribution to the low-frequency conductance σ_{dc} by the Einstein formula $\sigma_{dc} = e^2N(\varepsilon_F)$ D. Here $D = v_F^2\tau$ is the diffusion coefficient and τ is the transport lifetime. It is clear that the density of surface states $N(\varepsilon_F)$ at the Fermi energy also defines the contribution of the surface conductance to the total tunneling conductance in Weyl semimetals. As for the distributions of spin degrees of freedom, the bulk states for one Dirac point in a Weyl semimetal resemble chiral quasi-spin configurations in graphene, whereas surface states in a Weyl semimetal are analogues of helicoidal distributions of spin orientations in topological insulators. The energy spectrum and spin texture of surface states can be experimentally studied using the tunneling spectroscopy for which the behavior of the density of surface states is key. To separate surface contributions from bulk ones, to find the differences and to control the electron transport of surface carriers of different topological nature, we should follow the approach of [51].

The answer to the question which properties of the model under consideration are general and are inherent to other Weyl semimetals with violated spatial inversion symmetry can be as follows. The key properties controlling the hyperbolic dispersion dependence (8) and the Fermi-arc structure are the crystal symmetry and time-reversal symmetry (compare with [52]). In the case at hand (8), the character of the Fermi-arc dispersion is a consequence of the existence of the second-order axis, when arcs formed by rotation about this axis and after the time-reversal operation coincide [47]. It is now not difficult to imagine the arc structure in systems with different point groups [47, 52].

Certainly, the Fermi-arc dispersion in systems with spatial-inversion symmetry reflects features of situations when time-reversal symmetry is in some way violated. What properties of the density of states in this case and in the case considered in the present study are general? The above-mentioned observation of the behavior of the density of states in the intermediate energy range $\varepsilon_1 < \varepsilon < \varepsilon_2$, where it is almost constant as a result of embedding one-dimensional Fermi arches into two-dimensional momentum space, leads to the following assumption. The behavior of the energy dependence of the density of states in this intermediate region will be qualitatively the same as in systems with violated spatial-inversion symmetry.

It should be noted that we calculated the surface-state density in Weyl semimetals with violated spatial inversion and showed that it has a logarithmic singularity at $\varepsilon \to 0$, slowly decreases in the intermediate region, and tends to zero at $\varepsilon \to 1$ according to the law $\sqrt{2(1-\varepsilon)}$. In the intermediate energy region, this is reminiscent of the behavior of the density of states in a composition of two orthogonal Dirac metals immersed into two-dimensional space.

ACKNOWLEDGMENTS

We are grateful to Ch.L. Kane, M. Büttiker, V.Ya. Demikhovskii, S.V. Eremeev, E.R. Kocharovskaya, and V.G. Tyuterev for helpful discussions. We are also thankful to O.A. Shagalova who was involved in the study at an early stage, supported in part by the Russian Foundation for Basic Research, project no. 14-02-00174 and published in the Proceedings of the 28th International Symposium on Surface Physics (March, 22–28, 2015, Les Arcs, France).

E.V. Chulkov acknowledges the support of the Russian Foundation for Basic Research (project no. 13-02-12110), Saint Petersburg State University (project no. 11.50.202.2015), and the University of San Sebastian (grant no. IT-756-13).

REFERENCES

1. M. Z. Hasan and C. L. Kane, Rev. Mod. Phys. **82**, 3045 (2010).
2. X.-L. Qi and S.-C. Zhang, Rev. Mod. Phys. **83**, 1057 (2011).
3. J. E. Moore, Nature **464**, 194 (2010).
4. X. Chen, Z.-C. Gu, and X.-G. Wen, Phys. Rev. B **82**, 155138 (2010).
5. D. Culcer, E. H. Hwang, T. D. Stanescu, and S. Das Sarma, Phys. Rev. B **82**, 155457 (2010).
6. J. H. Bardarson and J. E. Moore, Rep. Prog. Phys. **76**, 056501 (2013).
7. J. E. Moore, Y. Ran, and X.-G. Wen, Phys. Rev. Lett. **101**, 186805 (2008).
8. A. Roth, C. Brüne, H. Buhmann, L. W. Molenkamp, J. Maciejko, X.-L. Qi, and S.-C. Zhang, Science **325**, 294 (2009).
9. J. Botimer, D. J. Kim, S. Thomas, T. Grant, Z. Fisk, and Jing Xia, arXiv:1211.6769.
10. C. L. Kane and E. J. Mele, Phys. Rev. Lett. **95**, 226801 (2005).
11. B. A. Bernevig, T. L. Hughes, and S.-C. Zhang, Science **314**, 1757 (2006).
12. M. König, S. Wiedmann, C. Brüne, A. Roth, H. Buhmann, L. W. Molenkamp, X.-L. Qi, and S.-C. Zhang, Science **318**, 766 (2007).
13. M. König, H. Buhmann, L. W. Molenkamp, T. Hughes, C.-L. Liu, X.-L. Qi, and S.-C. Zhang, J. Phys. Soc. Jpn. **77**, 031007 (2008).
14. G. Tkachov and E. M. Hankiewicz, Phys. Status Solidi B **250**, 215 (2013).
15. M. Büttiker, Phys. Rev. B **38**, 9375 (1988).
16. M. Büttiker, IBM J. Res. Dev. **32**, 317 (1988).
17. J. Wang, B. Lian, H. Zhang, and S.-C. Zhang, arXiv: 1306.1817.

18. C. Brüne, A. Roth, H. Buhmann, E. M. Hankiewicz, L. W. Molenkamp, J. Maciejko, X.-L. Qi, and S.-C. Zhang, Nature Phys. **8**, 485 (2012).
19. C. Brüne, A. Roth, E. G. Novil, M. König, H. Buhmann, E. M. Hankiewicz, W. Hanke, J. Sinova, and L. W. Molenkamp, Nature Phys. **6**, 448 (2010).
20. B. Zhou, H.-Z. Lu, R.-L. Chu, S.-Q. Shen, and Q. Niu, Phys. Rev. Lett. **101**, 246807 (2008).
21. C. Gils, S. Trebst, A. Kitaev, A. Ludwig, M. Troyer, and Z. Wang, Nature Phys. **5**, 834 (2009).
22. G. E. Volovik, *The Universe in a Helium Droplet* (Clarendon, Oxford, 2003).
23. X. Wan, A. M. Turner, A. Vishwanath, and S. Y. Savrasov, Phys. Rev. B **83**, 205101 (2011).
24. S.-Y. Xu, I. Belopolski, N. Alidoust, M. Neupane, C. Zhang, R. Sankar, S.-M. Huang, C.-C. Lee, G. Chang, B. K. Wang, G. Bian, H. Zheng, D. S. Sancez, A. Bansil, F. Chou, H. Lin, S. Jia, and M. Z. Hasan, arXiv:1502.03807 (2015).
25. S.-M. Huang, I. Belopolski, C.-C. Lee, G. Chang, B. K. Wang, N. Alidoust, G. Bian, M. Neupane, A. Bansil, H. Lin, and M. Z. Hasan, arXiv:1501.00755 (2015).
26. A. A. Burkov and L. Balents, Phys. Rev. Lett. **107**, 127205 (2011).
27. G. Y. Cho, arXiv:1110.1939 (2011).
28. A. P. Schnyder, S. Ryu, A. Furusaki, and A. W. W. Ludwig, Phys. Rev. B **78**, 195125 (2008).
29. A. P. Schnyder, S. Ryu, A. Furusaki, and A. W. W. Ludwig, AIP Conf. Proc. **1134**, 10 (2009); arXiv:0905.2029 (2009).
30. A. Kitaev, AIP Conf. Proc. **1134**, 22 (2009); arxiv:0901.2686 (2009).
31. B.-J. Yang and N. Nagaosa, Nature Commun. **5**, 4898 (2014).
32. A. A. Zyuzin and A. A. Burkov, Phys. Rev. B **86**, 115133 (2012).
33. P. Hosur and X.-L. Qi, arXiv:1401.2762 (2014).
34. K.-Y. Yang, Y.-M. Lu, and Y. Ran, Phys. Rev. B **84**, 075129 (2011).
35. M. Lv and S.-C. Zhang, Int. J. Mod. Phys. B **27**, 1350177 (2013).
36. I. Panfilov, A. A. Burkov, and D. A. Pesin, arXiv:1404.4890 (2014).
37. D. T. Son and B. Z. Spivak, Phys. Rev. B **88**, 104412 (2013).
38. S. A. Parameswaran, T. Grover, D. A. Abanin, D. A. Pesin, and A. Vishwanath, Phys. Rev. X **4**, 031035 (2014).
39. K.-Y. Yang, Y.-M. Lu, and Y. Ran, Phys. Rev. B **84**, 075129 (2011).
40. G. Y. Cho, J. H. Bardarson, Y.-M. Lu, and J. E. Moore, Phys. Rev. B **86**, 214514 (2012).
41. P. Hosur and X.-L. Qi, Compt. Rend. Phys. **14**, 857 (2013).
42. A. M. Turner and A. Vishwanath, arXiv:1301.0330 (2013).
43. P. Hosur, Phys. Rev. B **86**, 195102 (2012).
44. P. E. C. Ashby and J. P. Carbotte, arXiv:1310.2223 (2013).
45. E. V. Gorbar, V. A. Miransky, I. A. Shovkovy, and P. O. Sukhachov, arXiv:1407.1323 (2014).
46. G. B. Halasz and L. Balents, Phys. Rev. B **85**, 035103 (2012).
47. T. Ojanen, Phys. Rev. B **87**, 245112 (2013).
48. J. C. Y. Teo, and C. L. Kane, Phys. Rev. B **89**, 085101 (2014).
49. T. Neupert, C. Chamon, C. Mudry, and R. Thomale, arXiv:1403.0953 (2014).
50. Q. D. Gibson, D. Evtushinsky, A. N. Yaresko, V. B. Zabolotnyy, M. N. Ali, M. K. Fuccillo, J. van den Brink, B. Büchner, R. J. Cava, and S. V. Borisenko, arXiv:1405.0402 (2014).
51. H. Cao, C. Liu, J. Tian, Y. Xu, I. Miotkowski, M. Z. Hasan, and Y. P. Chen, arXiv:1409.3217 (2014).
52. R. Okugawa and S. Murakami, arXiv:1402.7145 (2014).

Translated by A. Kazantsev